Entropy Generation Analysis of MHD Casson Fluid over a Permeable Rotating Disk with Variable Fluid Properties and Heat Source

Shalini Jain[1], Ranjana Kumari[2]

[1,2] Department of Mathematics, University of Rajasthan, Jaipur-302004. INDIA.

Abstract—The main concern of this article is to analyze entropy generation for a steady laminar incompressible flow of MHD Casson fluid through porous medium over a permeable rotating disk with temperature dependent fluid properties. The governing non-linear PDEs are transformed into non-linear ODEs using appropriate similarity transformations. The obtained equations have been solved by RK-4 method with shooting technique using MATLAB. This study explores the effect of numerous physical parameters as Casson parameter, magnetic parameter, Prandtl number, relative temperature difference parameter, Forchheimer number, suction parameter, heat generation/absorption parameter on velocity profiles along radial, tangential and axial direction and temperature profile as well. Results are narrated and exhibited through graphs and tables.

Keywords—MHD, Casson fluid, porous medium, heat generation/absorption, rotating disk, entropy generation.

I.INTRODUCTION

Flow due to rotating disk has wide range of applications in many practical aspects in engineering and industrial process. Some examples of utilizations are such as in food processing industries, aircrafts, engines, turbomachinary, multipower distributors manipulative, centrifugal pumps, gas turbines and power generating systems, computer devices, oceanography, viscometer, rotational air cleaning systems and medical equipments etc. Primarily Karman [1] closely investigated the fluid flow due to rotating disk and he gave the similarity transformations for rotating disk flow. After him several researchers extended and used Karman's study as a reference. Study of MHD laminar fluid flow between a fixed impermeable disk and a porous rotating disk have been done by Kavenuke et. al. [2]. Steady fluid flow over a rotating disk of a viscous fluid in porous medium have been examined by Attia [3]. Jana et. al. [4] have been studied a hydrodynamic flow in porous medium between two non-coincident rotating disks. Yin et. al. [5] have been investigated the flow of nanofluids over a rotating disk geometry with uniform stretching rate in the radial direction. Uddin et. al. [6] have been analyzed the steady MHD flow of nanofluids. They have taken into account heat generation/absorption over rotating disk. A numerical study of MHD Casson fluid due to rotating disk considering effect of thermophoresis and Brownian motion have been done by Rehman et. al. [7]. Verma et.al. [8] have been analyzed the Soret effect of MHD flow over a porous rotating disk. Recently fluid flow over rotating disk considering presence of chemical reaction have been studied by several researchers [9–11].

MHD was first studied by Alfven [12]. MHD flow has various applications in astrophysics, aerospace, nuclear reactors etc. MHD flow in porous medium is extremely useful in optimization of solidification process of metals, alloys, biological systems, irrigation problems, textile and polymer industries etc. Casson fluid is type of non- Newtonian fluid which acts like an elastic solid less than yield stress and after it starts flowing. Bhattacharyya [13] has been studied MHD stagnation point flow of Casson fluid in the presence of thermal radiation over a stretching sheet. Casson fluid flow over exponentially stretching surface has been explored by Pramanik [14]. Casson fluid over an unsteady stretching surface have been analyzed by Mukhopadhyay et.al. [15]. Sarojamma et.al. [16] have been examined MHD Casson fluid flow in a vertical channel. MHD Casson fluid have been studied by Pushapalatha et. al. [17] with convective boundary conditions. Radiation and chemical reaction parallelly examined for MHD Casson fluid over oscillating vertical plate in porous medium by Kataria and Patel [18].

Mondal et.al. [19] have been explored the flow of Casson fluid considering variable viscosity and they also consider effect of variable thermal conductivity. Asogwa and Ibe [20] have been studied MHD Casson fluid with heat and mass transfer over a permeable stretching sheet. Entropy is related with disorder of a system and surroundings. Heat is renowned reason for entropy generation. Due to presence of heat some additional movements come out which are liable for deficit in energy. For example, friction, internal displacement of molecules of fluid, vibration of molecules etc. By analyzation of entropy generation we can modernize and enhance the performance of system of devices which are based on concept of mechanics, thermodynamics etc. Bejan [21] was the first who reported study on entropy generation. After him several researchers extended his work. Venkateswar and Bhaskar [22] have been analyzed entropy generation of MHD Casson fluid flow with convective boundary conditions in micro channel. Entropy generation of MHD Casson fluid have investigated by Sohail et. al. [23] over a non-linear stretching surface in the presence of Joule heating and thermal radiation. Usman et. al. [24] have been studied second law analysis of micropolar nanofluid with MHD and Radiation which is non-linear over a rotating and stretching disk. After reviewing the literature, we noted that entropy generation analysis of MHD Casson fluid over porous rotating disk with variable fluid properties have not been studied yet. Therefore, the current investigation aims to fill this slot in the literature. This study explores the effect of numerous physical

parameters on velocity profiles along radial, tangential and axial direction and temperature profile as well. Results are narrated and exhibited through graphs and tables.

II.MATHEMATICAL FORMULATION

A steady incompressible slip flow of Casson fluid through porous medium over a permeable rotating disk in the presence of external magnetic field has been considered. Disk of radius r is placed at z = 0 in cylindrical polar coordinate system rotating with constant angular velocity Ω. u, v, w are the velocities of Casson fluid in the directions r, θ, φ respectively. B_0 is uniform magnetic field. T_W is the uniform temperature of the rotating disk's surface. $T$and P are the temperature and pressure of the fluid respectively. T_∞ and P_∞ (T_W>T_∞) are the temperature and pressure of the surrounding fluid.

Following [25], the fluid properties μ (viscosity), k (thermal conductivity) and ρ (density) are assumed to be function of temperature.

$$\mu = \mu_\infty (T/T_\infty)^a$$
$$k = k_\infty (T/T_\infty)^b \qquad (1)$$
$$\rho = \rho_\infty (T/T_\infty)^c$$

Here, a, b, c are randomly choosen exponents. For ideal gas $a = 0.7$, $b = 0.83$, $c = -0.1$. μ_∞, $k_\infty$and ρ_∞ are the uniform fluid properties.

The governing flow equation in cylindrical polar coordinates for axisymmetric flow are-

$$\frac{\partial(\rho r u)}{\partial r} + \frac{\partial(\rho r w)}{\partial z} = 0 \qquad (2)$$

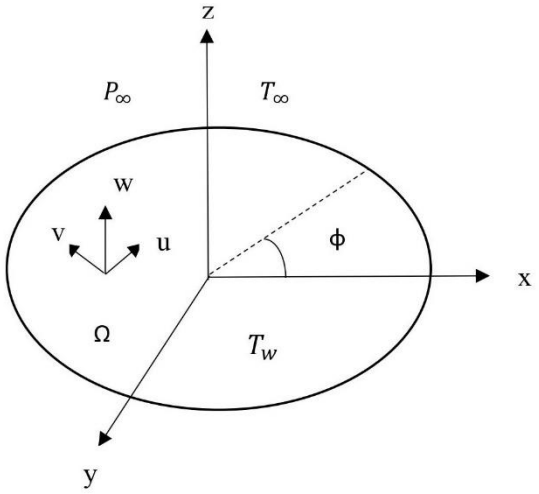

Fig. 1: FLOW DIAGRAM OF THE MODEL

$$u\frac{\partial u}{\partial r} + w\frac{\partial u}{\partial z} - \frac{v^2}{r} = -\frac{1}{\rho}\frac{\partial P}{\partial r} + \frac{1}{\rho}\left(1+\frac{1}{\lambda}\right)\left[\frac{\partial}{\partial r}\left(\mu\frac{\partial u}{\partial r}\right) + \frac{\partial}{\partial r}\left(\mu\frac{u}{r}\right) + \frac{\partial}{\partial z}\left(\mu\frac{\partial u}{\partial z}\right)\right] - \frac{\mu u}{\rho k^*} - F^* u^2 - \frac{\sigma B_0^2 u}{\rho} \qquad (3)$$

$$u\frac{\partial v}{\partial r} + w\frac{\partial v}{\partial z} + \frac{uv}{r} = \frac{1}{\rho}\left(1+\frac{1}{\lambda}\right)\left[\frac{\partial}{\partial r}\left(\mu\frac{\partial v}{\partial r}\right) + \frac{\partial}{\partial r}\left(\mu\frac{v}{r}\right) + \frac{\partial}{\partial z}\left(\mu\frac{\partial v}{\partial z}\right)\right] - \frac{\mu v}{\rho k^*} - F^* v^2 - \frac{\sigma B_0^2 v}{\rho} \qquad (4)$$

$$u\frac{\partial w}{\partial r} + w\frac{\partial w}{\partial z} = -\frac{1}{\rho}\frac{\partial P}{\partial z} + \frac{1}{\rho}\left(1+\frac{1}{\lambda}\right)\left[\frac{\partial}{\partial r}\left(\mu\frac{\partial w}{\partial r}\right) + \frac{1}{r}\frac{\partial}{\partial r}(\mu w) + \frac{\partial}{\partial z}\left(\mu\frac{\partial w}{\partial z}\right)\right] - \frac{\mu w}{\rho k^*} - F^* w^2 \qquad (5)$$

$$u\frac{\partial T}{\partial r} + w\frac{\partial T}{\partial z} = \frac{1}{\rho C_p}\left[\frac{\partial}{\partial r}\left(k\frac{\partial T}{\partial r}\right) + \frac{k}{r}\frac{\partial T}{\partial r} + \frac{\partial}{\partial z}\left(k\frac{\partial T}{\partial z}\right)\right] + \frac{Q}{\rho C_p}(T - T_\infty) \qquad (6)$$

Where, λ is Casson parameter, k^* is permeability of porous media, Q is heat generation/absorption coefficient, C_b is drag factor, $F^* = \frac{C_b}{r k^{*\frac{1}{2}}}$ is non-uniform inertia factor. Under the boundary conditions [25]-

at $z = 0$, $\quad u = \frac{2-\sigma_v}{\sigma_v}\lambda\frac{\partial u}{\partial z}$

$$v = r\Omega + \frac{2-\sigma_v}{\sigma_v}\lambda\frac{\partial v}{\partial z}$$

$$w = w_0$$

$$T = T_w + \frac{2-\sigma_t}{\sigma_t}\frac{2\beta}{1+\beta}\frac{\lambda}{Pr}\frac{\partial T}{\partial z}$$

at $z \to \infty, \quad u \to 0, v \to 0, T \to T_\infty$.

Where, σ_v, σ_t represents tangential momentum and energy accommodation coefficient respectively, A is mean free path, β is ratio of specific heats.

To convert the governing flow boundary layer equations in non-dimensional form Von-Karman's similarity transformations are-

$$\eta = (\frac{\Omega}{\nu_\infty})^{\frac{1}{2}} r,$$
$$u = \Omega r F(\eta),$$
$$v = \Omega r G(\eta),$$
$$w = (\Omega \upsilon_\infty)^{\frac{1}{2}} H(\eta), \qquad (7)$$
$$P - P_\infty = \mu_\infty \Omega P(\eta),$$
$$\theta(\eta) = \frac{T - T_\infty}{T_w - T_\infty}$$

ν_∞ stands for uniform kinematic viscosity. F, G, H, θ are non- dimensional functions of η. Employing above transformations (7), for equation (2), (3), (4), and (6) we get the following system of non-dimensional equations-

$$\left(1+\frac{1}{\lambda}\right)[F'' + a\varepsilon\theta' F'(1+\epsilon\theta)^{-1}] - KF - (1+\epsilon\theta)^{c-a}[Fr\, F^2 + MF(1+\epsilon\theta)^{-C} + F^2 + HF' - G^2 = 0$$
(8)

$$\left(1+\frac{1}{\lambda}\right)[G + a\varepsilon\theta' G'(1+\epsilon\theta)^{-1}] - KG - (1+\epsilon\theta)^{c-a}[Fr\, G^2 + MG(1+\epsilon\theta)^{-C} + 2FG + HG' = 0 \quad (9)$$

$$H' + c\varepsilon H\theta'^{(1+\epsilon\theta)^{-1}} + 2F = 0 \qquad (10)$$

$$\theta'' + b\varepsilon(1+\epsilon\theta)^{-1}\theta'^2 + [\delta\theta - H\theta'](1+\epsilon\theta)^{c-b} = 0 \qquad (11)$$

Bc's- at $\eta = 0$,

$$F(0) = \gamma F'(0), G(0) = 1 + \gamma G'(0),$$
$$\theta(0) = 1 + \xi\theta'(0), H(0) = W_s \qquad (12)$$

At $\eta \to \infty, F(\eta) \to 0, G(\eta) \to 0, \theta(\eta) \to 0$

Where, $K = \frac{\nu_\infty}{k^*\Omega}, Fr = \frac{C_b}{k^{*\frac{1}{2}}}, M = \frac{\sigma B_0^2}{\rho_\infty \Omega}, Pr = \frac{\mu_\infty C_p}{k_\infty}$ and $\delta = \frac{Q}{\Omega\rho C_p}$ are the porosity parameter, Forchheimer number, magnetic parameter, Prandtl number and heat generation absorption parameter respectively. $\varepsilon = \frac{\Delta T}{T_\infty}$, stands for relative temperature difference parameter. It takes values positive, negative and zero according heated, cooled and constant temperature surface.

Ratio of mean free path to fluid particle diameter is denoted as Knudsen number $Kn = \frac{A}{r}$. For present problem Kn is taken between 0.001 to 0.1 (for slip flow).

$Re = \frac{\Omega r^2}{\nu_\infty}$, denotes rotational Reynolds number. Range considered for present study is 0 to 1000.

$\gamma = \frac{2-\sigma_v}{\sigma_v} Kn\sqrt{Re}$ and $\xi = \frac{2-\sigma_t}{\sigma_t}\frac{2\beta}{1+\beta}\frac{Kn}{Pr}\sqrt{Re}$ are slip and temperature jump factor both varying from 0 to 12. W_s is suction parameter. We considered $\sigma_v = \sigma_t = 0.9$ and $\beta = 1.4$.

III.SOLUTION

The non-linear ODE's have been solved using Runge-Kutta scheme together with shooting technique. Non-dimensional ODE's are reduced to the following system of IVP-

Let $F = f_1, F' = f_2, G = f_3, G' = f_4, H = f_5,$
$\theta = f_6, \theta' = f_7,$

$$f_1' = f_2$$
$$f_2' = (1+\frac{1}{\lambda})^{-1}[Kf_1 + (1+\varepsilon f_6)^{c-a}\{Fr f_1^2 + Mf_1(1+\varepsilon f_6)^{-c} + f_1^2 + f_2 f_5 - f_3^2\} - \left(1+\frac{1}{\lambda}\right)a\varepsilon f_2 f_7(1+\varepsilon f_6)^{-1}]$$
$$f_3' = f_4$$
$$f_4' = (1+\frac{1}{\lambda})^{-1}[Kf_3 + (1+\varepsilon f_6)^{c-a}\{Fr f_3^2 + Mf_3(1+\varepsilon f_6)^{-c} + f_1^2 + 2f_1 f_3 + f_4 f_5\} - \left(1+\frac{1}{\lambda}\right)a\varepsilon f_4 f_7(1+\varepsilon f_6)^{-1}]$$
(13)

$$f_5' = -c\varepsilon f_5 f_7(1+\varepsilon f_6)^{-1} - 2f_1$$

$$f_6' = f_7$$

$f_7' = -b\varepsilon f_7^2(1+\varepsilon f_6)^{-1} + [f_5 f_7 - (1+ \quad \varepsilon f_6)^{-c}\delta f_6]Pr(1+\varepsilon f_6)^{c-b}$

Bc's- at $\eta = 0$, $f_1(0) = \gamma f_2(0), f_2(0) = s_1$,

$$f_3(0) = 1 + \gamma f_4(0), f_4(0) = s_2,$$

$$f_5(0) = W_s, f_6(0) = 1 + \xi f_7(0), \quad f_7(0) = s_3,$$

At $\eta \to \infty, f_1(\eta) \to 0, f_3(\eta) \to 0, f_6(\eta) \to 0$.

Particular case: taking fluid properties constant,

$$\mu = \mu_\infty(\frac{T}{T_\infty})^a = \mu_\infty(\frac{T_\infty + \Delta T\theta}{T_\infty})^a = \mu_\infty(1+\varepsilon\theta)^a$$

Taking $\varepsilon = 0, \mu = \mu_\infty$,

Similarly at $\varepsilon = 0$, $\rho = \rho_\infty, k = k_\infty$

Thus for constant fluid properties non-dimensional ODE's are reduced in the form-

$$\left(1+\frac{1}{\lambda}\right)F'' - KF - [FrF^2 + MF + F^2 + HF' - G^2 = 0$$

$$\left(1+\frac{1}{\lambda}\right)G'' - KG - [FrG^2 + MG + 2FG + HG' = 0$$

$$H' + 2F = 0$$

$$\theta'' + \delta Pr\theta - PrH\theta' = 0$$

And boundary conditions remain unaltered.

Skin friction coefficient: Along radial direction, $Cf_r = \frac{\tau_r}{\rho U^2}$ (14)

Along tangential direction, $Cf_r = \frac{\tau_r}{\rho U^2}$ (15)

Where, U is linear velocity of the disk. And the stress components along both directions following [26] are given as by equation (16) and (17) respectively-

$$\tau_r = \left(1+\frac{1}{\lambda}\right)\left[\mu\left(\frac{\partial u}{\partial z} + \frac{\partial w}{\partial r}\right)\right]_{z=0}$$

$$= \left(1+\frac{1}{\lambda}\right)(1+\varepsilon)^a \Omega\mu_\infty Re^{\frac{1}{2}}F'(0) \quad (16)$$

$$\tau_t = \left(1+\frac{1}{\lambda}\right)\left[\mu\left(\frac{\partial v}{\partial z} + \frac{1}{r}\frac{\partial w}{\partial \phi}\right)\right]_{z=0}$$

$$= \left(1+\frac{1}{\lambda}\right)(1+\varepsilon)^a \Omega\mu_\infty Re^{\frac{1}{2}}G'(0) \quad (17)$$

Utilizing above values of stresses from equations (16) and (18) in equations (14) and (15) we have the following non dimensional components of skin friction coefficients-

$$(1+\varepsilon)^{c-a}\sqrt{Re}Cf_r = \left(1+\frac{1}{\lambda}\right)F'(0) \quad (18)$$

$$(1+\varepsilon)^{c-a}\sqrt{Re}Cf_t = \left(1+\frac{1}{\lambda}\right)G'(0) \quad (19)$$

Nusselt number: the coefficient of heat transfer in non- dimensional form is-

$$Nu = \frac{rq_w}{k_\infty(T_w - T_\infty)} \quad (20)$$

$q_w = -(k\frac{\partial T}{\partial z})_{z=0}$

Taking together the above both expressions with similarity transformations, we have Nusselt number Nu as equation (21)-

$$(1+\varepsilon)^{-b}Re^{\frac{-1}{2}}Nu = -\theta'(0) \quad (21)$$

IV.ENTROPY

Following [27, 28] the production of entropy is defined as,

$$S'''_{gen} = \frac{k}{T_\infty^2}\left(\frac{\partial T}{\partial z}\right)^2 + \frac{\mu}{T_\infty}\left(1+\frac{1}{\lambda}\right)[2\left\{\left(\frac{\partial u}{\partial r}\right)^2 + \frac{u^2}{r^2} + \left(\frac{\partial w}{\partial z}\right)^2\right\} + \left(\frac{\partial v}{\partial z}\right) + \left(\frac{\partial u}{\partial z}\right) + r(\frac{\partial}{\partial r}\left(\frac{v}{r}\right))^2] + \frac{\sigma B_0^2}{T_\infty}(u^2+v^2) \quad (22)$$

non-dimensional form, after employing transformations [7]-

$$N_G = \varepsilon(1+\varepsilon\theta)^b f_7^2 + (1+\varepsilon\theta)^a \frac{Br}{Re}\left(1+\frac{1}{\lambda}\right)[2\{2f_1^2 - c\varepsilon f_5 f_7(1+\varepsilon\theta)^{-1} - 2f_1\} + Re(f_2^2+f_4^2)] + MBr(f_1^2+f_3^2) \quad (23)$$

$$Be = \varepsilon(1+\varepsilon\theta)^b f_7^2 / N_G \quad (24)$$

where, $N_G = \frac{S'''_{gen} T_\infty \nu_\infty}{k_\infty \Omega \Delta T}$, non-dimensional entropy generation rate, $Br = \frac{\mu_\infty \Omega^2 r^2}{k_\infty \Delta T}$ is Brinkman number, Be is Bejan number representing ratio of entropy production caused by thermal irreversiblity to entire rate of entropy production.

V.RESULTS AND ANALYSIS

We have plotted the graphs taking $M = 0.5, K = -1, Kn = 0.05, \delta = -0.1, Fr = 0.1, Pr = 1, Re = 100$ $W_s = -1$ $, \lambda = 0.2$ standard values. Fig. [2-5] denotes the effect of Casson Parameter on velocities in radial, tangential and axial direction and temperature profile. It is depicted that enhancement in Casson parameter reduce the radial velocity and temperature profile. Physically it means Casson parameter reduces boundary layer thickness. We noted that velocity near to the surface of disk is greater than away from the axis of disk.Fig.4 shows increase in Casson Parameter leads to increase in axial velocity. Fig.[6-8] represent the influence of magnetic parameter on velocities. It is noted that increase in magnetic parameter leads to decrease in velocity components in radial, tangential and axial direction. It is because high magnetic field increase the temperature of the flow near rotating disk so a resistive force called Lorentz force produced which resist flow.

Effects of suction parameter on velocity components and temperature have been depicted through Fig.[9-12].We have noticed that enhancement in suction parameter W_s bring about decrement in all velocity components and temperature as well. Because due to suction fluid enters into porous surface of disk therefore velocity and thermal boundary layer become thinner.

Fig.[13-16] report the effect of heat generation (when $\delta > 0$) /absorption (when $\delta < 0$) parameter and also comparison for both variable and constant fluid properties . We perceived that thermal boundary layer as well as velocities upgraded with an increase in δ. Fig.[17] denotes increasing Prandtl number reduces temperature profile. Fig.[18-21] characterize the consequences of Knudsen number on velocities and temperature distributions and also it shows comparison for constant and variable fluid properties. In case of slip flow Knudsen number lies between 0.001 and 0.1. Temperature and velocity components show same behaviour i.e. decrement with increasing Knudsen number. Fig.[22-24] illustrate the effect of diversification of Forchheimer number Fr on velocities in radial, tangential and axial directions. It is observed that increasing Forchheimer number reduces all components of velocities and for constant fluid properties peak shifted downwards than variable fluid properties.

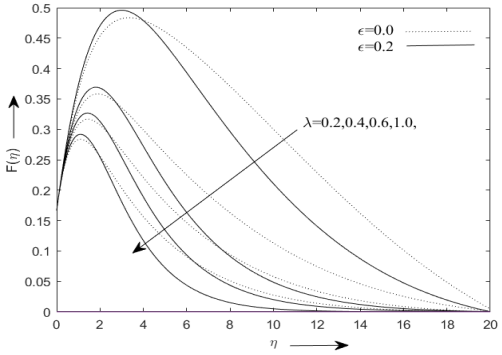

*Fig.*2: RADIAL VELOCITY FOR VRYING CASSON PARAMETER

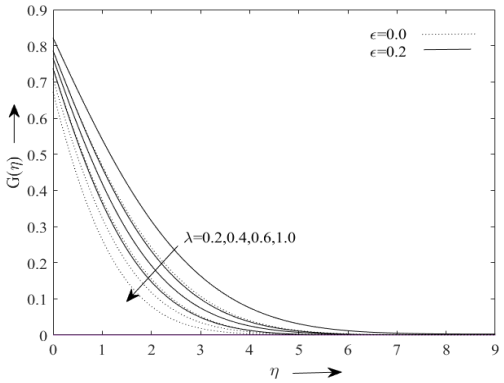

Fig. 3: TANGENTIAL VELOCITY FOR VARYING CASSON PARAMETER

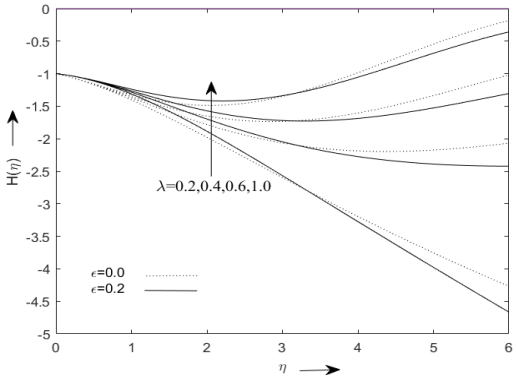

Fig. 4:AXIAL VELOCITY FOR VARYING CASSON PARAMETER

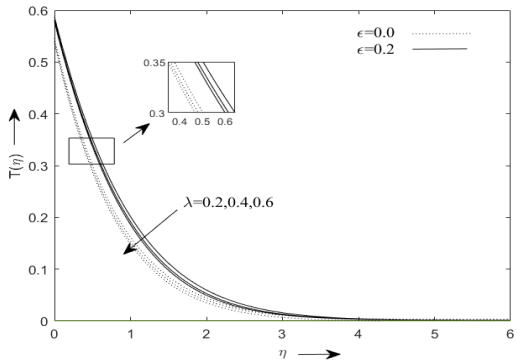

Fig.5: TEMPERATURE PROFILE FOR VARYING CASSON PARAMETER

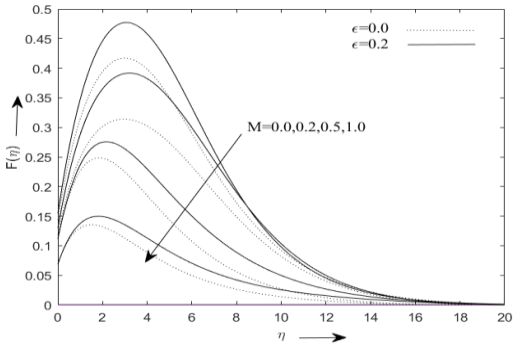

*Fig.6:*RADIAL VELOCITY FOR VARYING MAGNETIC PARAMETER

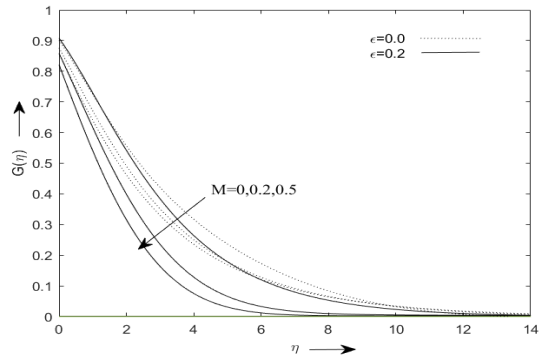

Fig.7:TANGENTIAL VELOCITY FOR VARYING MAGNETIC PARAMETER

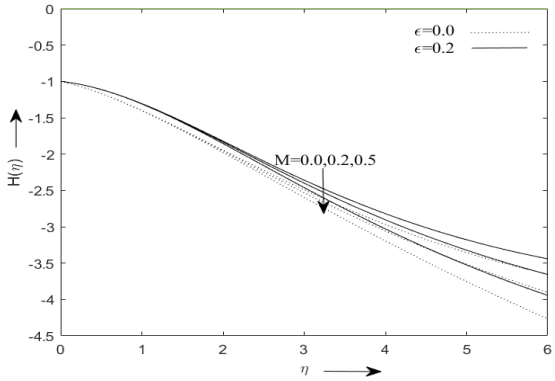

Fig.8:AXIAL VELOCITY FOR VARYING MAGNETIC PARAMETER

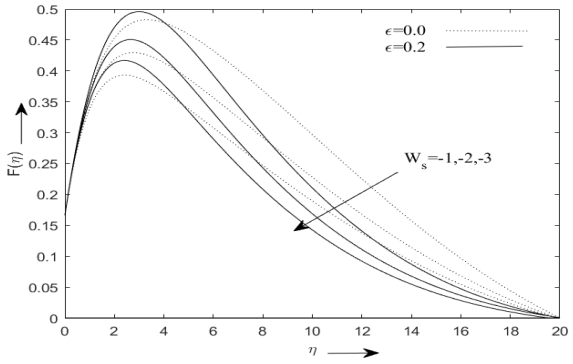

Fig.9: RADIAL VELOCITY FOR VARYING SUCTION PARAMETER

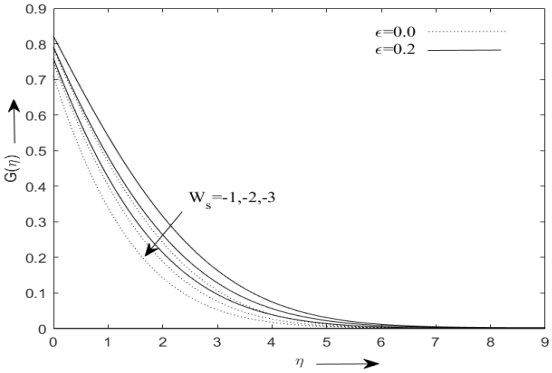

Fig.10: TANGENTIAL VELOCITY FOR VARYING SUCTION PARAMETER

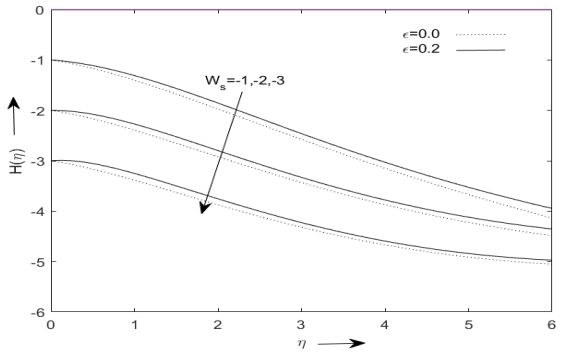

*Fig. 11:*AXIAL VELOCITY FOR VARYING SUCTION PARAMETER

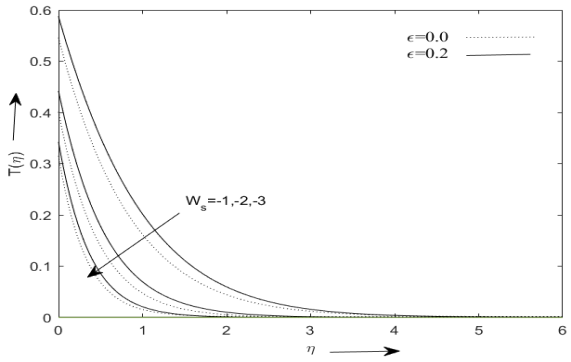

*Fig.12:*TEMPERATURE PROFILE FOR VARYING SUCTION PARAMETER

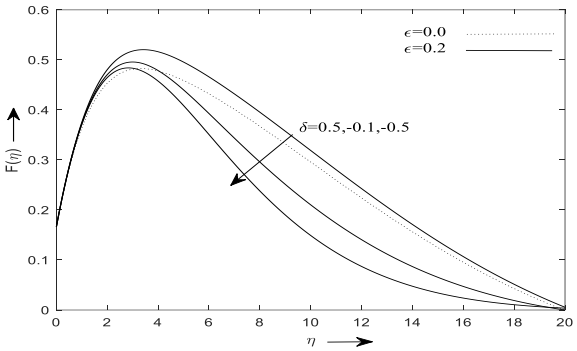

*Fig.13:*RADIAL VELOCITY FOR VARYING HEAT GENERATION /ABSORPTION PARAMETER

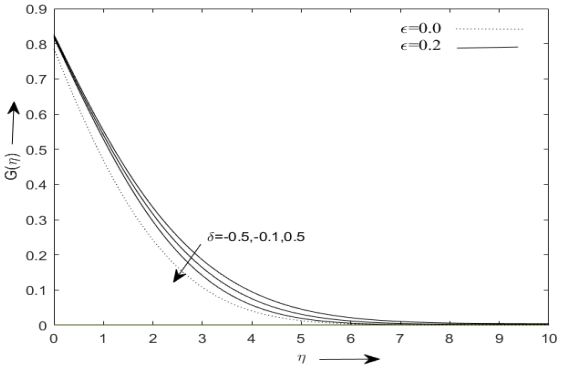

*Fig.14:*TANGENTIALVELOCITY FOR VARYING HEAT GENERATION /ABSORPTION PARAMETER

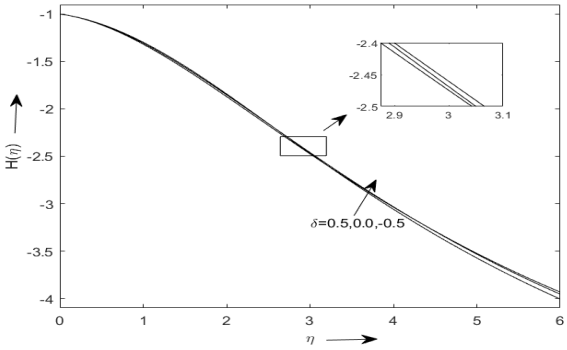

Fig.15: AXIAL VELOCITY FOR VARYING HEAT GENERATION /ABSORPTION PARAMETER

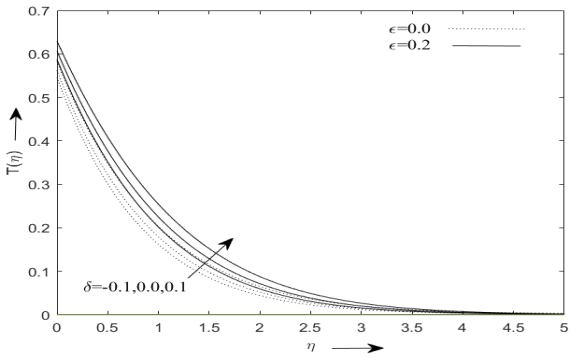

Fig.16:TEMPERATURE PROFILE FOR VARYING HEAT GENERATION /ABSORPTION PARAMETER

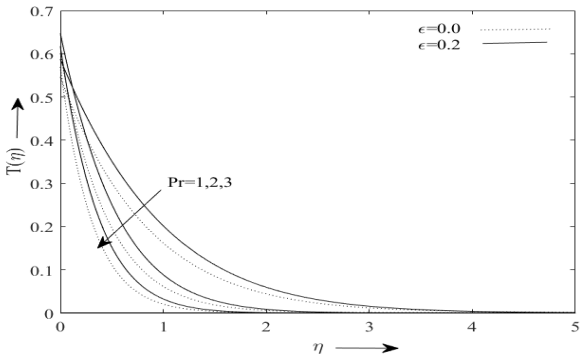

*Fig. 17:*TEMPERATURE PROFILE FOR VARYING PRANDTL NUMBER

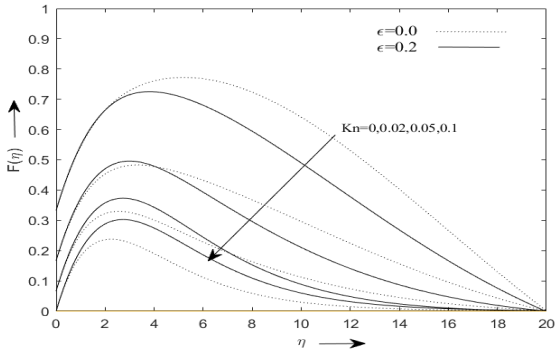

*Fig.18:*RADIAL VELOCITY FOR VARYING KNUDSEN NUMBER

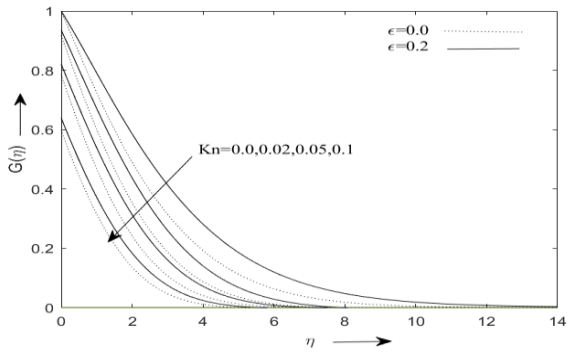

Fig. 19:TANGENTIAL VELOCITY FOR VARYING KNUDSEN NUMBER

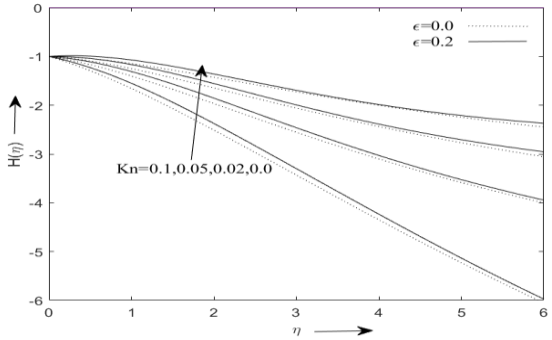

Fig.20:AXIAL VELOCITY FOR VARYING KNUDSEN NUMBER

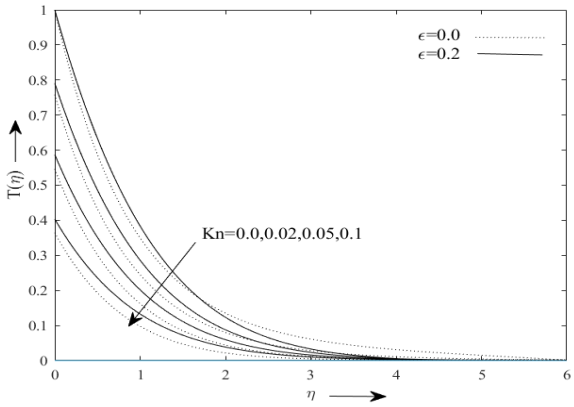

Fig.21:TEMPERATURE PROFILE FOR VARYING KNUDSEN NUMBER

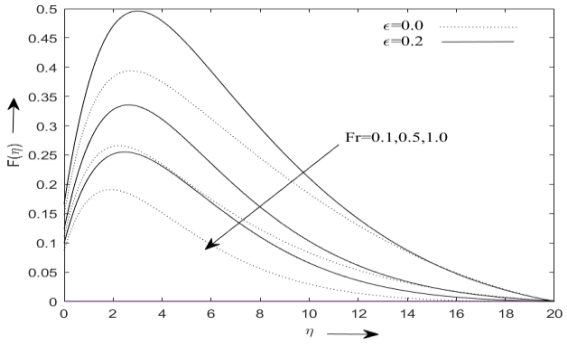

Fig.22:RADIAL VELOCITY FOR VARYING FORCHHEIMER NUMBER

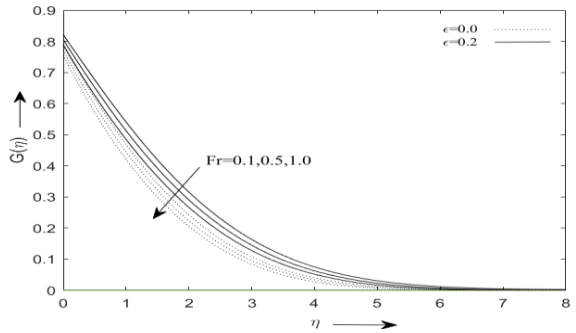

Fig. 23:TANGENTIAL VELOCITY FOR VARYING FORCHHEIMER NUMBER

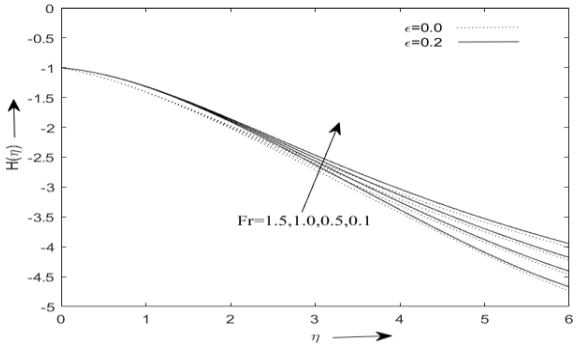

Fig24: AXIAL VELOCITY FOR VARYING FORCHHEIMER NUMBER

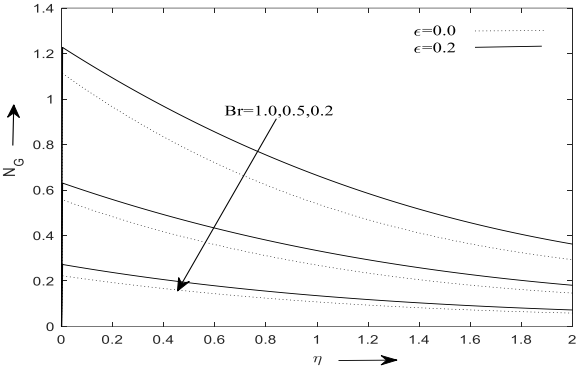

Fig.25:ENTROPY GENERATION NUMBER FOR VARYING BRINKMAN NUMBER

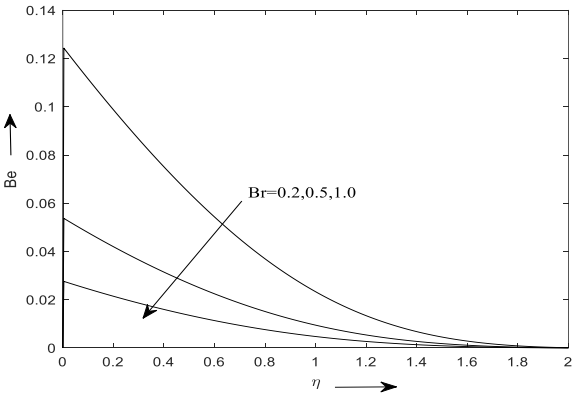

Fig. 26: BEJAN NUMBER FOR VARYING BRINKMAN NUMBER

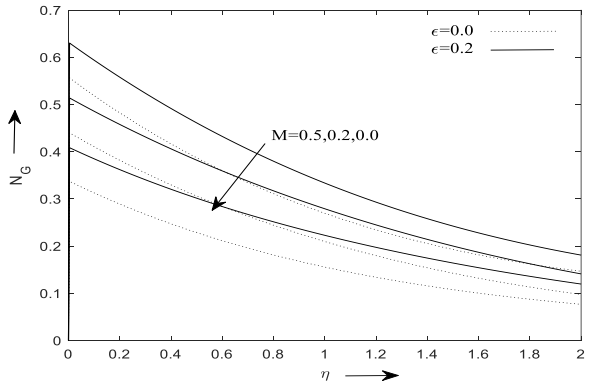

*Fig.27:*ENTROPY GENERATION NUMBER FOR VARYING MAGNETIC PARAMETER

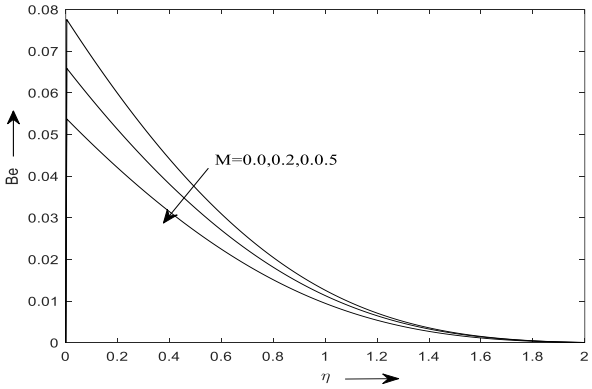

*Fig. 28:*ENTROPY GENERATION NUMBER FOR VARYING BRINKMAN NUMBER

Fig.[25-26] interpret the variation of entropy generation number N_G and Bejan number Be for brinkman number Br respectively.We know that Bejan number is directly associated with viscous dissipation and directly proportional to it. So increment in Br enhance entropy production. Fig.[25] shows that for constant fluid properties graph is shifted downwards. Fig.[27-28] illustrate the effect of magnetic parameter on entropy generation number and Bejan number respectively. We noticed that Bejan number reduces with increasing M. Increase in M physically leads to irreversibility effect to fluid friction and generate Lorentz force and it causes increase in entropy generation.

Table [2]-[4] represents the validation of present result with previous literature [29,30] by comparison of skin friction coefficient and Nusselt number. The value of λ is taken 10000 here for validation. Table [1] shows results of $F'(0), -G'(0)$ and $-\theta'(0)$ for present investigation taking $\mathrm{K} = -1, \lambda = 0.2, \mathrm{Kn} = 0.05, \delta = -0.1, \mathrm{Fr} = 0.1, \mathrm{Pr} = 1, \mathrm{Re} = 100, \mathrm{M} = 0.5$ with temperature difference parameter ε. We observe that with increasing ε, $F'(0)$increases while $-G'(0)$ and $-\theta'(0)$decreases.

ε	$F'(0)$	$-G'(0)$	$-\theta'(0)$
0.0	0.070915552	0.556105575	0.643323259
0.1	0.073687470	0.51506340	0.615018615
0.2	0.076701098	0.463727197	0.587184148
0.3	0.079961483	0.416026421	0.560149127

Table 1VALUES OF $F'(0), -G'(0), -\theta'(0)$ FOR VARIATION IN TEMPERATURE DIFFERENCE PARAMETER.

W_s	$F'(0)$		
	Present	[29]	[30]
-2	0.24282	0.24241310	0.242421
-1	0.38978	0.38954065	0.389569
0	0.51013	0.51022378	0.510233
1	0.48949	0.48948057	0.489481

Table 2 COMPARISION OF $F'(0)$ FOR $K = Kn = M = \delta = \varepsilon = Fr = 0, Pr = 0.71$ and $\lambda \to \infty$.

W_s	$-G'(0)$		
	Present	[29]	[30]
-2	2.03690	2.03859590	2.038527
-1	1.17519	1.17526180	1.175222
0	0.61594	0.61592380	0.615922
1	0.30218	0.30217432	0.302173

Table 3 COMPARISION OF -G'(0) FOR $K = Kn = M = Fr = \delta = \varepsilon = 0, Pr = 0.71$ AND $\lambda \to \infty$.

W_s	$-\theta'(0)$		
	Present	[29]	[30]
-2	1.43579	1.43876482	1.437782
-1	0.79101	0.79393633	0.793048
0	0.32595	0.32637889	0.325856
1	0.08492	0.08504687	0.084884

Table 4 COMPARISION OF $-\theta'(0)$ FOR $K = Kn = M = Fr = \delta = \varepsilon = 0, Pr = 0.71$ AND $\lambda \to \infty$.

VI.CONCLUSIONS

In this investigation we have studied Casson fluid over a permeable rotating disk considering both variable as well as constant fluid properties. We described the results through graphs and tables. And have find following conclusions-

- Velocities and temperature profiles decrease with Casson parameter.
- All velocity components decrease with magnetic parameters as well as with Forchheimer number.
- Heat generation/absorption parameter increase velocities as well as temperature.
- Suction parameter and Knudsen parameter have same effect i.e. decrease the velocity and temperature.
- Entropy generation number shows directly proportional behaviour with Brinkman number and magnetic parameter while reverse effect is observed for Bejan number.

References

[1] T. Von Karm´ an, "Uber laminare und turbulente reibung," ´ Z. *Angew. Math. Mech.*, vol. 1, pp. 233–252, 1921.

[2] D. Kavenuke, E. Massawe, and O. D. Makinde, "Modeling laminar flow between a fixed impermeable disk and a porous rotating disk," *African Journal of Mathematics and Computer Science Research*, vol. 2, no. 7, pp. 157–162, 2009.

[3] H. Attia, "Steady flow over a rotating disk in porous medium with heat transfer," *Nonlinear Analysis: Modelling and Control*, vol. 14, no. 1, pp. 21–26, 2009.

[4] R. Jana, M. Maji, S. Das, S. L. Maji, and S. K. Ghosh, "Hydrodynamic flow between two non-coincident rotating disks embedded in porous media," *World Journal of Mechanics*, vol. 1, no. 2, pp. 50–56, 2011.

[5] C. Yin, L. Zheng, C. Zhang, and X. Zhang, "Flow and heat transfer of nanofluids over a rotating disk with uniform stretching rate in the radial direction," *Propulsion and Power Research*, vol. 6, no. 1, pp. 25–30, 2017.

[6] Z. Uddin, R. Asthana, M. K. Awasthi, and S. Gupta, "Steady MHD flow of nano-fluids over a rotating porous disk in the presence of heat generation/absorption: a numerical study using pso," *J. Appl. Fluid Mech*, vol. 10, no. 3, pp. 871–879, 2017.

[7] K. U. Rehman, M. Malik, W. A. Khan, I. Khan, and S. O. Alharbi, "Numerical solution of non-Newtonian fluid flow due to rotatory rigid disk*," Symmetry*, vol. 11, no. 5, p. 699, 2019.

[8] K. Verma, D. Borgohain, and B. Sharma, "Soret effect through a rotating porous disk of mhd fluid flow," *Int. J. Innov. Technol. Explor. Eng*, vol. 9, pp. 21–28, 2020.

[9] M. Asma, W. Othman, and T. Muhammad, "Numerical study for Darcy– Forchheimer flow of nanofluid due to a rotating disk with binary chemical reaction and Arrhenius activation energy," *Mathematics*, vol. 7, no. 10, p. 921, 2019.

[10] N. Tarakaramu and P. Satya Narayana, "Chemical reaction effects on bioconvection nanofluid flow between two parallel plates in rotating system with variable viscosity: a numerical study," *Journal of Applied and Computational Mechanics*, vol. 5, no. 4, pp. 791–803, 2019.

[11] T. Mehmood, M. Ramzan, F. Howari, S. Kadry, and Y.-M. Chu, "Application of response surface methodology on the nanofluid flow over a rotating disk with autocatalytic chemical reaction and entropy generation optimization," *Scientific Reports*, vol. 11, no. 1, pp. 1–18, 2021.

[12] H. Alfven, "Existence of electromagnetic-hydrodynamic waves," ´ *Nature*, vol. 150, no. 3805, pp. 405–406, 1942.

[13] K. Bhattacharyya, "MHD stagnation-point flow of Casson fluid and heat transfer over a stretching sheet with thermal radiation," *Journal of thermodynamics*, vol. 2013, 2013.

[14] S. Pramanik, "Casson fluid flow and heat transfer past an exponentially porous stretching surface in presence of thermal radiation," *Ain Shams Engineering Journal*, vol. 5, no. 1, pp. 205–212, 2014.
[15] S. Mukhopadhyay, P. R. De, K. Bhattacharyya, and G. Layek, "Casson fluid flow over an unsteady stretching surface," *Ain Shams Engineering Journal*, vol. 4, no. 4, pp. 933–938, 2013.
[16] G. Sarojamma, B. Vasundhara, and K. Vendabai, "Mhd casson fluid flow, heat and mass transfer in a vertical channel with stretching walls," *Int. J. Sci and Innovative Mathhematical Res*, vol. 2, no. 10, pp. 800–810, 2014.
[17] K. Pushpalatha, V. Sugunamma, J. R. Reddy, and N. Sandeep, "Heat and mass transfer in unsteady MHD Casson fluid flow with convective boundary conditions," *International Journal of Advanced Science and Technology*, vol. 91, pp. 19–38, 2016.
[18] H. R. Kataria and H. R. Patel, "Radiation and chemical reaction effects on MHD Casson fluid flow past an oscillating vertical plate embedded in porous medium," *Alexandria Engineering Journal*, vol. 55, no. 1, pp. 583–595, 2016.
[19] R. K. Mondal, P. P. Gharami, S. F. Ahmmed, S. Arifuzzaman et al., "A simulation of Casson fluid flow with variable viscosity and thermal conductivity effects," *Mathematical Modelling of Engineering Problems*, pp. 625–633, 2019.
[20] K. Asogwa and A. Ibe, "A study of MHD Casson fluid flow over a permeable stretching sheet with heat and mass transfer," *J. Eng. Res. Rep.*, vol. 10, p. 25, 2020.
[21] A. Bejan, "Second-law analysis in heat transfer and thermal design," *Advances in heat transfer. Elsevier*, 1982, vol. 15, pp. 1–58.
[22] M. Venkateswarlu and P. Bhaskar, "Entropy generation and bejan number analysis of MHD Casson fluid flow in a micro-channel with Navier slip and convective boundary conditions," *International Journal of Thermo fluid Science and Technology*, vol. 7, 2020.
[23] M. Sohail, Z. Shah, A. Tassaddiq, P. Kumam, and P. Roy, "Entropy generation in MHD Casson fluid flow with variable heat conductance and thermal conductivity over non-linear bi-directional stretching surface," *Scientific Reports*, vol. 10, no. 1, pp. 1–16, 2020.
[24] A. Ghaffari, I. Mustafa, T. Muhammad, Y. Altaf et al., "Analysis of entropy generation in a power-law nanofluid flow over a stretchable rotatory porous disk," *Case Studies in Thermal Engineering*, vol. 28, p. 101370, 2021.
[25] S. Jain and S. Bohra, "Radiation effects in flow through porous medium over a rotating disk with variable fluid properties," *Advances in Mathematical Physics*, vol. 2016, 2016.
[26] A. Maleque, "Unsteady MHD non-Newtonian Casson fluid flow due to a porous rotating disk with uniform electric field," *Fluid Mech Open Acc*, vol. 3, no. 123, pp. 2476–2296, 2016.
[27] M. M. Rashidi and N. F. Mehr, "Effects of velocity slip and temperature jump on the entropy generation in magnetohydrodynamic flow over a porous rotating disk," *Journal of Mechanical engineering*, vol. 1, no. 3, pp. 4–14, 2012.
[28] N. Freidoonimehr, M. M. Rashidi, S. Abelman, and G. Lorenzini, "Analytical modelling of MHD flow over a permeable rotating disk in the presence of Soret and Dufour effects: entropy analysis," *Entropy*, vol. 18, no. 5, p. 131, 2016.
[29] M. Alam, N. Poddar, M. Rahman, and K. Vajravelu, "Transient hydromagnetic forced convective heat transfer slip flow due to a porous rotating disk with variable fluid properties," *American Journal of Heat and Mass Transfer*, vol. 2, no. 3, pp. 165–189, 2015.
[30] N. Kelson and A. Desseaux, "Note on porous rotating disk flow," *ANZIAM Journal*, vol. 42, pp. C837–C855, 2000.